Inorganic Chemistry

Article

pubs.acs.org/IC

A Complexation Study of 2,6-Bis(1-(*p*-tolyl)-1*H*-1,2,3-triazol-4-yl)pyridine Using Single-Crystal X-ray Diffraction and TRLFS

Claude Kiefer,[†] Anna. T. Wagner,[†] Björn B. Beele,[‡,§] Andreas Geist,[§] Petra J. Panak,*[,‡,§] and Peter W. Roesky*[,†]

[†]Institut für Anorganische Chemie, Karlsruher Institut für Technologie, Engesserstr. 15, 76131 Karlsruhe, Germany

[‡]Physikalisch-Chemisches Institut, Ruprecht-Karls-Universität Heidelberg, Im Neuenheimer Feld 253, 69120 Heidelberg, Germany

[§]Institut für Nukleare Entsorgung, Karlsruher Institut für Technologie, P.O. Box 3640, 76021 Karlsruhe, Germany

Supporting Information

ABSTRACT: To develop a selective ligand for the separation of lanthanides(III) and actinides(III) the coordination chemistry of the chelating N-donor ligand 2,6-bis(1-(*p*-tolyl)-1*H*-1,2,3-triazol-4-yl)pyridine (BTTP) was investigated. The two isostructural lanthanide compounds $[Ln(BTTP)_3(OTf)_3]$ (Ln = Eu (**1**), Sm (**2**); OTf = trifluoromethanesulfonate) were synthesized and fully characterized. The solid-state structures of both compounds were established by single-crystal X-ray diffraction. The complexation of Cm(III) and Eu(III) with BTTP in acetonitrile was studied using time-resolved laser fluorescence spectroscopy. With increasing BTTP concentration Cm(III) 1:2 and 1:3 complexes and Eu(III) 1:1 and 1:3 complexes are identified. The conditional stability constants of the 1:3 complex species with BTTP are log β_3 = 14.0 for Cm(III) and log β_3 = 10.3 for Eu(III). Both M(III) 1:3 complexes are prone to decomplexation with increasing acidity.

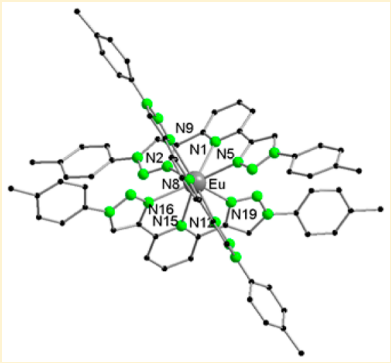

INTRODUCTION

In 2013, 9.7% of the world's electricity was supplied by nuclear power plants,[1] annually producing 10 500 tons of used nuclear fuel,[2] which must be disposed of finally. Different countries pursue different strategies for doing so, that is, by direct disposal of the fuel or disposal of only the vitrified highly active waste remaining after reprocessing by the PUREX process. This process separates uranium and plutonium, to be used for the fabrication of fresh nuclear fuel. Currently, strategies are under investigation to separate and recycle not only uranium and plutonium but also the so-called minor actinides, neptunium, americium, and curium, with a focus on americium. The minor actinides are recovered from a PUREX raffinate by selective extraction.[3,4] The implications of this strategy are the subject of several studies.[5,6]

These strategies at some point require separating trivalent actinides, An(III) = Am(III), Cm(III) from the chemically similar lanthanides, Ln(III), generated by nuclear fission. Oxygen-donor ligands are not selective for An(III) over Ln(III); however, soft nitrogen- or sulfur-donor ligands display a more or less pronounced selectivity for An(III) over Ln(III).[7−14] Further to a high affinity toward An(III) the complexing agent should meet several other requirements such as high stability against nitric acid and radiation, fast extraction kinetics, and solubility of both the agent and its extracted complexes in the organic phase to minimize the possibility of third-phase formation or precipitation. Additionally, the agent must be able to extract metal ions from nitric acid solutions of low pH to avoid hydrolysis of actinide ions.

Well-established examples for such complexing agents are the 2,6-bis(1,2,4-triazin-3-yl)pyridine (BTP) ligands (Scheme 1),

Scheme 1. Molecular Structure of the Alkylated 2,6-Ditriazinylpyridines

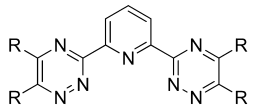

R = CH_3, C_2H_5, *n*-C_3H_7, *i*-C_3H_7, *n*-C_4H_9, *i*-C_4H_9

first reported by Case et al. in 1971.[15] Later Kolarik et al. reported the first solvent-extraction studies with alkylated BTP ligands. These ligands selectively extract Am(III) and Cm(III) over Ln(III) cations with separation factors for Am(III) over Eu(III) higher than 100 under acidic conditions.[16] On the basis of the tridentate BTP ligands, tetradentate 6,6′-bis(1,2,4-triazin-3-yl)-2,2′-bipyridine (BTBP) and 6,6′-bis(1,2,4-triazin-3-yl)-1,10-phenanthroline (BTPhen) ligands were developed and investigated.[17−22]

Despite further studies having been performed with BTP ligands, a comprehensive understanding of such ligand selectivity is still missing on a molecular level. To understand and optimize the complexation and extraction properties of BTP-type ligands, some structural changes were performed on

Received: April 9, 2015
Published: July 13, 2015

DOI: 10.1021/acs.inorgchem.5b00803
Inorg. Chem. 2015, 54, 7301−7308

this system, including alkylation of the substituents on the pyridine[23,24] or at the molecule periphery[24−26] and modifications in the lateral rings (Scheme 1).[24,27−33]

On the basis of our experience with derivatives of the BTP ligand, such as 2,6-(tetrazol-5-yl)-2,2′-bipyridine (HN4bipy),[34] 6-(3,5-dimethyl-1*H*-pyrazol-1-yl)-2,2′-bipyridine (dmpbipy),[28] and 2,6-bis-[5-(2,2-dimethylpropyl)-1*H*-pyrazol-3-yl]pyridine (C5-BPP)[29,31] (Scheme 2), we focused our work on further

Scheme 2. Molecular Structures of HN_4bipy,[34] dmpbipy,[28] C5-BPP,[13,14] and BTTP

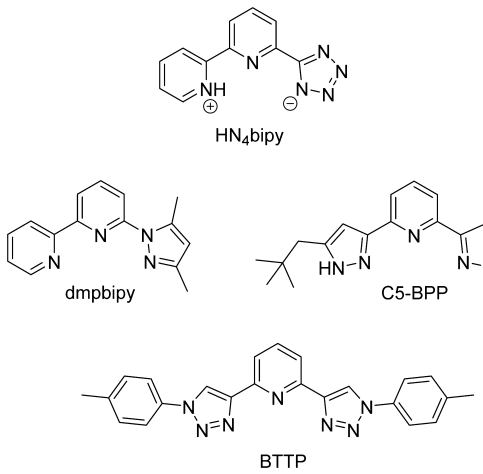

modification of the triazinyl moieties of the BTP backbone. Inspired by a report of Limberg and Hecht et al.,[35] who synthesized a polyglycol-substituted 2,6-bis(triazolyl)pyridine Eu(III) complex and investigated its luminescence properties, we report the application of 2,6-bis(1-(*p*-tolyl)-1*H*-1,2,3-triazol-4-yl)pyridine (BTTP) ligand (Scheme 2) for the separation of actinides(III) from lanthanides(III). BTTP is a nitrogen-rich variation of the C5-BPP ligand with the pyrazolyl units being replaced by triazolyl rings further substituted by *p*-tolyl groups. We report the synthesis and characterization of Eu(III) and Sm(III) BTTP complexes as well as the relevant thermodynamic data for the complex formation of BTTP with Cm(III) and Eu(III). These data were determined by time-resolved laser fluorescence spectroscopy (TRLFS). TRLFS is a highly sensitive spectroscopic method suitable for the characterization and quantification of complex species in the sub-micromolar concentration range. The complexation of Cm(III) and Eu(III) with a broad range of polydentate N-donor ligands has already been studied using TRLFS and reported.[27,36,32,28,34,29,30,37,38] Finally, liquid−liquid extraction tests were performed to study the extraction performance of BTTP.

EXPERIMENTAL SECTION

Synthesis. All solvents as well as copper(II) sulfate (Sigma-Aldrich, 98% ACS reagent), europium(III)trifluoromethanesulfonate (ABCR), *L*-(+)-sodium ascorbate (Sigma-Aldrich), and samarium(III)-trifluoromethanesulfonate (Alfa Aesar) were used as purchased from commercial sources without further purification. Deuterated solvents were obtained from Aldrich (99 atom % D). 4-Azidotoluene and 2,6-diethynylpyridine were prepared according to the literature procedure.[39]

NMR spectra were recorded on a Bruker Avance II 300 MHz or Avance 400 FT spectrometer. Chemical shifts are referenced to internal solvent resonances and are reported relative to tetramethylsilane (^{1}H and ^{13}C NMR). IR spectra were obtained on a Bruker Tensor 37 FT IR spectrometer. Electrospray ionization mass spectrometry (ESI-MS) spectra were recorded on Bruker MicroTOF and IonSpec FT-ICR (7 T) ESI-MS spectrometers. Electron ionization mass spectrometry (EI-MS) spectra were recorded on a Thermofischer DFS sector field spectrometer. Elemental analyses were performed with a Vario EL or Microcube of Elementar Analysensysteme GmbH.

Synthesis of 2,6-Bis(1-(*p*-tolyl)-1*H*-1,2,3-triazol-4-yl)-pyridine.[39] A mixture of *p*-tolyl azide (0.100 g, 0.751 mmol) and 2,6-diethynylpyridine (0.047 g, 0.375 mmol) was dissolved in 5 mL of dimethylformamide. $CuSO_4{\cdot}5H_2O$ (0.037 g, 0.150 mmol) and sodium ascorbate (0.030 g, 0.150 mmol) were added, and the solution was stirred at ambient temperature for 48 h. The reaction mixture was poured into water (100 mL) and extracted three times with CH_2Cl_2 (60 mL). The combined organic phases were washed with water and dried (Na_2SO_4). The solvent was removed to afford 0.117 g of BTTP (97%) as a colorless solid. Single crystals suitable for X-ray structure determination were grown from a saturated dichloromethane solution.

^{1}H NMR (deuterated dimethyl sulfoxide (DMSO-d_6)): δ, ppm = 9.33 (s, 2H, triazole-H), 8.08 (s, 3H, pyridine-H), 7.89 (d, 4H, Ph-H), 7.48 (d, 4H, Ph-H), 2.42 (s, 6H, CH_3). ^{13}C{^{1}H} NMR (DMSO-d_6): δ, ppm = 149.5, 148.2, 138.7, 138.6, 134.3, 130.3, 121.7, 120.2, 118.8, 20.6. Anal. Calcd for $C_{23}H_{19}N_7$: C, 70.21, H, 4.87; N, 24.92. Found C, 70.18; H, 4.88; N, 24.60%. MS: found 393.407; $C_{23}H_{19}N_7$ requires 393.170.[39]

General Synthetic Procedure for [Ln(BTTP)$_3$(OTf)$_3$]; Ln = Eu (1), Sm (2).[40] A mixture of BTTP (3 equiv) and Ln(OTf)$_3$ (1 equiv; Ln = Eu, Sm) was dissolved in tetrahydrofuran (THF), and the resulting solution was stirred for 24 h at room temperature; a light yellow solid started to precipitate after several minutes. The solid was collected by filtration, washed with THF, and dried in vacuo.

*[Eu(BTTP)$_3$(OTf)$_3$] (**1**).* By using 200 mg of BTTP (0.508 mmol) and 101 mg of Eu(OTf)$_3$ (0.169 mmol), the product was isolated as yellow powder (190 mg, 63%). Slow diffusion of diethyl ether into a saturated solution of **1** in acetonitrile induced formation of crystals of **1** suitable for single-crystal X-ray analysis.

IR (ATR): $\tilde{\nu}$ (cm^{-1}) = 2963 (w), 1518 (vw), 1470 (vw), 1412 (vw), 1260 (s), 1091 (s), 1019 (s), 865 (w), 798 (vs), 705 (w), 638 (w). ESI-MS (CH_3CN): m/z = [$C_{69}H_{57}EuN_{21}^{3+}$] calcd. 444.1439; found 444.1337.

*[Sm(BTTP)$_3$(OTf)$_3$] (**2**).* By using 100 mg (0.254 mmol) of BTTP and 51 mg (0.085 mmol) of Sm(OTf)$_3$ the product was isolated as yellow powder (81 mg, 54%). Slow diffusion of diethyl ether into a saturated solution of **2** in acetonitrile induced formation of crystals of **2** suitable for single-crystal X-ray analysis.

IR (ATR): $\tilde{\nu}$ (cm^{-1}) = 3098 (vw), 2960 (w), 2923 (w), 2853 (w), 1617 (w), 1587 (w), 1517 (m), 1469 (m), 1408 (w), 1258 (vs), 1224 (m), 1146 (m), 1097 (m), 1073 (m), 1043 (m), 1029 (vs), 994 (m), 981 (w), 864 (w), 816 (s), 800 (vs); 754 (w), 705 (w), 669 (w), 637 (vs), 572 (m), 563 (m), 516 (s). ESI-MS (CH_3CN): m/z = 443.8194 [$C_{69}H_{57}SmN_{21}^{3+}$] calcd. 443.8096; found 443.8194.

X-ray Crystallographic Studies of 1 and 2. A suitable crystal was covered in mineral oil (Aldrich) and mounted onto a glass fiber. The crystal was transferred directly to a N_2 cold stream of a Stoe IPDS 2 or a Stoe Stadivari diffractometer. All structures were solved by direct or Patterson methods (SHELXS-97).[41] The remaining non-hydrogen atoms were located from successive difference Fourier map calculations. The refinements were executed by using full-matrix least-squares techniques on F^2, minimizing the function $(F_0 - F_c)^2$, where the weight is defined as $4F_o^2/2(F_o^2)$ and F_o and F_c are the observed and calculated structure factor amplitudes using the program SHELXL-97.[41] Carbon-bound hydrogen atom positions were calculated. The hydrogen atom contributions were calculated but not refined. The locations of the largest peaks in the final difference Fourier map calculations, as well as the magnitude of the residual electron densities, in each case were of no chemical significance.

*Crystal Data for **1**.* $C_{69}H_{57}EuN_{21}$ $3CF_3O_3S$, M = 1776.54, triclinic, a = 13.6887(10) Å, b = 16.4306(12)Å, c = 18.810(2) Å, α = 71.259(6)°, β = 88.315(6)°, γ = 88.557(6), V = 4004.1(5) Å^3, T = 100(2) K, space group $P\bar{1}$, Z = 2, μ = 0.95 mm^{-1}, 37 880 reflections measured, 15 768 independent reflections (R_{int} = 0.1394). The final R_1

DOI: 10.1021/acs.inorgchem.5b00803
Inorg. Chem. 2015, 54, 7301−7308

Scheme 3. Synthesis of the Ligand System BTTP[39]

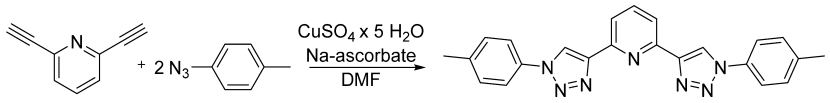

Scheme 4. Synthesis of [Ln (BTTP)$_3$(CF$_3$SO$_3$)$_3$] (Ln = Eu (1), Sm (2))

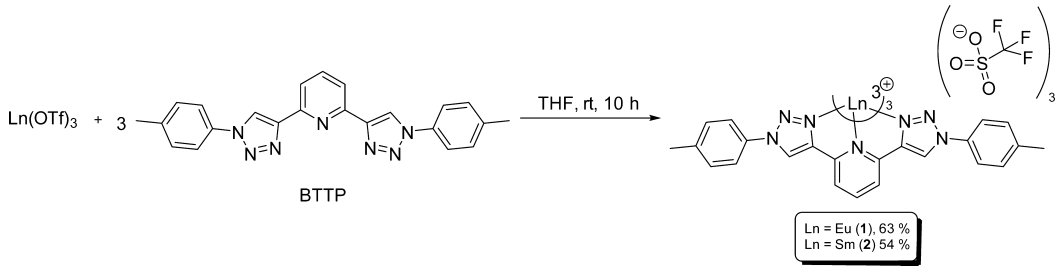

values were 0.0805 ($I > 2\sigma(I)$). The final $wR(F^2)$ values were 0.2009 (all data). The goodness of fit on F^2 was 0.986.

Crystal Data for **2**. $C_{69}H_{57}SmN_{21}$ $3CF_3O_3S$, M = 1779.52, triclinic, a = 13.746(3) Å, b = 16.440(3) Å, c = 18.795(4) Å, α = 71.08(3)°, β = 88.25(3)°, γ = 88.59(3)°, V = 4015(2) Å^3, T = 100(2) K. The X-ray data collected from **2** was very poor, but its composition was deduced from the difference Fourier map.

TRLFS Sample Preparation and Measurement. BTTP ligand solutions for TRLFS studies with Cm(III) and Eu(III) were prepared by dissolving 3.93 mg (1×10^{-5} mol) of BTTP in 10.0 mL of MeCN (5.0 vol % H_2O), resulting in a 1.0×10^{-3} mol L^{-1} stock solution, which was subsequently diluted to a 1.0×10^{-4} and a 5.0×10^{-5} mol L^{-1} solution when needed. The Cm(III) solution was prepared by adding 15 μL of an aqueous stock solution of $Cm(ClO_4)_3$ ([Cm(III)] = 6.7×10^{-6} mol L^{-1} in 0.01 mol L^{-1} $HClO_4$) to 35 μL of H_2O and 950 μL of MeCN, resulting in a 1.0×10^{-7} mol L^{-1} solution of Cm(III) in MeCN with a residual water content of 5.0 vol %. According to α spectroscopy and ICP-MS the isotopic mass distribution of the Cm(III) solution is 89.7% ^{248}Cm, 9.4% ^{246}Cm, and less than 0.5% ^{243}Cm, ^{244}Cm, ^{245}Cm, and ^{247}Cm. The Eu(III) solution was prepared by adding 44 μL of an aqueous stock solution of $Eu(ClO_4)_3$ ([Eu(III)] = 1.06×10^{-3} mol L^{-1} in 0.01 mol L^{-1} $HClO_4$) to 6 μL of H_2O and 950 μL of MeCN, resulting in a 4.0×10^{-5} mol L^{-1} solution of Eu(III) in MeCN (5.0 vol % H_2O).

Titrations were performed by stepwise addition of a BTTP solution in MeCN (5.0 vol % H_2O) to Cm(III) or Eu(III) solutions, respectively, in the same solvent mixture. The resulting mixture was allowed to equilibrate for 10 min before measurement, which had been shown in earlier studies to be sufficient for equilibration.

To determine the acid stability of Cm(III)- and Eu(III)-BTTP complexes, perchloric acid was added stepwise to equilibrated solutions of [Cm(BTTP)$_3$] and [Eu(BTTP)$_3$] in MeCN (5.0 vol % H_2O), according to earlier studies performed with other 1:3 M(III)−N−donor complex species.[32,30] A fluorescence spectrum was recorded after each titration step.

TRLFS Setup. TRLFS measurements were performed using a Nd:YAG-pumped dye laser system [Surelite II laser (Continuum), NARROWscan D-R dye laser (Radiant Dyes Laser Accessories)]. For Cm(III) excitation a wavelength of 396.6 nm and for Eu(III) excitation a wavelength of 394.0 nm was used. Fluorescence emissions were recorded at a 90° angle to the exciting laser beam. For spectral decomposition a Shamrock 303i spectrograph (ANDOR) equipped with a 300, 900, and 1200 lines/mm grating turret was used. The fluorescence emission was detected by an ICCD camera [iStar Gen III, A-DH 720 18F-63 (ANDOR)]. Before the fluorescence light was recorded, a delay time of 1.0 μs was used to discriminate short-lived fluorescence of organic ligands and Rayleigh scattering. The quartz cuvette was temperature-controlled at T = 25 °C.

Liquid−Liquid Extraction. The extracting performance of BTTP was determined by measuring the distribution of ^{241}Am(III) and ^{152}Eu(III) between an organic phase containing BTTP and an aqueous phase containing nitric acid. The distribution was determined both in presence and absence of the lipophilic anion source 2-bromodecanoic acid. ^{241}Am and ^{152}Eu are radionuclides with characteristic γ lines, which are easily detected by γ counting.

Organic phases were solutions of

(a) 1.0 mmol L^{-1} BTTP in 1-octanol or
(b) 1.0 mmol L^{-1} BTTP + 0.5 mol L^{-1} 2-bromodecanoic acid in 1-octanol.

The organic phases were prepared by dissolving appropriate amounts of BTTP and 2-bromodecanoic acid in the diluent. For solubility reasons, BTTP concentrations greater than 1.0 mmol L^{-1} could not be realized.

Aqueous phases were ^{241}Am(III) + ^{152}Eu(III) in HNO_3 (0.01/0.1/0.5/0.7/1.0/2.0 mol L^{-1}). They were prepared by adding 10 μL of a stock solution of 100 kBq/mL ^{241}Am(III) and 100 kBq/mL ^{152}Eu(III) in 0.1 mol L^{-1} HNO_3 to 490 μL of HNO_3 with concentrations given above.

Equal volumes of the organic and aqueous phases were brought into contact for 15 min at 20 °C using an orbital shaker (2500/min). Samples were centrifuged to separate the phases. Subsequently, ^{241}Am and ^{152}Eu activities were determined in 400 μL aliquots of each phase by γ counting (Packard Cobra Auto Gamma 5003).

RESULTS AND DISCUSSION

Synthesis of BTTP and Its Lanthanide Complexes (Ln = Eu (1), Sm (2)).[40] The ligand BTTP was synthesized by a $CuSO_4$-catalyzed Huisgen-type 1,3-dipolar cycloaddition from 4-azidotoluene and 2,6-diethynylpyridine referring to a literature procedure we recently published (Scheme 3).[39]

The coordination compounds [Ln(BTTP)$_3$(OTf)$_3$] (Ln = Eu (**1**), Sm (**2**)) were synthesized referring to literature procedure published by Limberg and Hecht et al.[35] The corresponding lanthanide triflate salts Ln(OTf)$_3$ (Ln = Eu (**1**), Sm (**2**)) were reacted with 3 equiv of BTTP in THF at room temperature (Scheme 4). After workup, subsequent diffusion of diethyl ether in a saturated solution of acetonitrile led to the formation of crystals suitable for single X-ray diffraction analysis. Compounds **1** and **2** were characterized by standard analytical and spectroscopic techniques. The solid-state structures were determined by single-crystal X-ray diffraction (Figure 1). Although the X-ray data collected from **2** was very poor, its composition was deduced from the difference Fourier map. The composition of **1** and **2** was also further established by ESI-MS (cf. Figure 3).

Both compounds crystallize in the triclinic space group $P\bar{1}$ with two molecules and three triflate anions in the unit cell.

DOI: 10.1021/acs.inorgchem.5b00803
Inorg. Chem. 2015, 54, 7301−7308

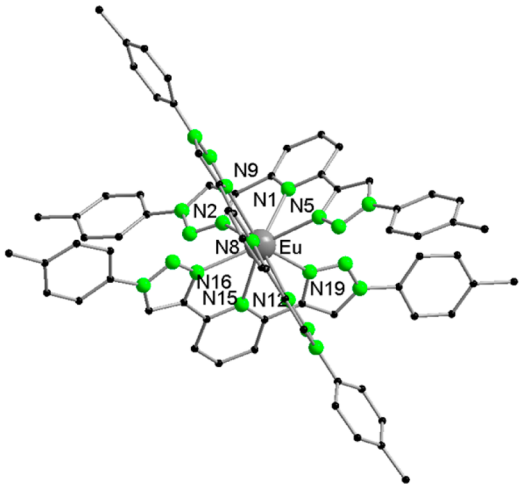

Figure 1. Solid-state structure of the $[Eu(BTTP)_3]^{3+}$ cation of **1**; the central metal is coordinated by nine nitrogen atoms (CN = 9). Hydrogen atoms, anions, and cocrystallized solvent molecules were omitted for clarity. The corresponding Sm compound (**2**) is isostructural but not shown herein, because of the poor quality of the X-ray data. Selected distances [Å] and angles [deg]: Eu–N1 2.597(7), Eu–N2 2.547(7), Eu–N5 2.505(7), Eu–N8 2.573(6), Eu–N9 2.579(6), Eu–N12 2.572(7), Eu–N15 2.594(6), Eu–N16 2.528(7), Eu–N19 2.510(7); N1–Eu–N2 64.0(2), N1–Eu–N5 64.2(2), N1–Eu–N8 121.2(2), N1–Eu–N9 75.1(2), N1–Eu–N12 134.6(2), N2–Eu–N5 128.1(2), N2–Eu–N8 135.3(2), N2–Eu–N9 76.7(2), N2–Eu–N12 148.2(2), N5–Eu–N8 73.0(2), N5–Eu–N9 87.5(2), N5–Eu–N12 77.4(2), N8–Eu–N9 64.3(2), N8–Eu–N12 64.1(2), N9–Eu–N12 128.4(2).

The central Ln(III) atom is coordinated by three BTTP ligands, and each of the ligands act as a three-dentate chelating ligand resulting in a total coordination number of nine (CN = 9) for the lanthanide atom. Each BTTP ligand coordinates with one nitrogen atom of the pyridine ring and one nitrogen atom of each triazolyl moiety directly to the lanthanide atom (Figure 1 and Supporting Information, Figure S1).

The coordinating nitrogen atoms of the triazolyl rings (altogether six) surround the metal atom in a trigonal prismatic shape, whereas the two triangular faces of the prism are not exactly eclipsed but are slightly staggered (see Figure 2a). The remaining nitrogen donor atoms of the pyridyl moieties form the three caps, which complete the total tricapped trigonal prismatic coordination geometry around the central metal atom (see Figure 2b).

The tricapped trigonal prismatic coordination geometry around lanthanide metal centers in complexes with BTP-type ligands is a common structural motif.[24,33,35] Comparing this structure with the related compound of $[Eu(L)_3](OTf)_3$ (L = 2,6-bis[1-(4-iodophenyl)-*1H*-1,2,3-triazol-4-yl]-4-(3,6,9-trioxadec-1-yloxy)pyridine),[35] it can be noted that the $Eu-N_{pyridyl}$ distances are very similar in the range of $d(Eu-N_{pyridyl})$ = 2.572–2.598 Å, whereas the $Eu-N_{triazolyl}$ in $[Eu(BTTP)_3]^{3+}$ are slightly longer than reported in $[Eu(L)_3]^{3+}$.

Both compounds were also characterized by ESI-MS from an acetonitrile solution. Despite the poor quality of the X-ray data of **2**, the composition of this compound could be clearly deduced by ESI-MS. In the positive ion spectrum of **2** the base peak at m/z = 443.8194 amu was assigned to triply charged cationic species $[Sm(BTTP)_3]^{3+}$ by spectrum simulation (Figure 3; see also Supporting Information, Figure S2 for compound **1**).

TRLFS Studies. In addition to the characterization of Ln(III) BTTP complexes using single-crystal X-ray analysis and ESI-MS, TRLFS studies were performed to get a thorough insight into the complexation performance of BTTP toward Cm(III) and Eu(III) as representatives for actinides(III) and lanthanides(III).

Cm(III) fluorescence spectra resulting from the $^6D'_{7/2} \rightarrow {}^8S'_{7/2}$ transition with increasing BTTP concentration are shown in Figure 4a. For better comparison the spectra are normalized to the same peak area. The emission band of the Cm(III) solvent complex species shows an emission maximum at λ_{max} = 600.7 nm. Hence, a distinct bathochromic shift in comparison to the shift of the Cm(III) aquo ion ($[Cm(H_2O)_9]^{3+}$, λ_{max} = 593.7 nm)[42] is observed. This shift results from the replacement of water by acetonitrile solvent molecules in the first coordination sphere. Two new emission bands are observed with increasing BTTP concentration. The emission band of the first Cm(III) complex species shows an emission maximum at λ_{max} = 607.1 nm. This emission band is only observable at 3.1 μmol $L^{-1} \leq$ [BTTP] $\leq$ 5.0 μmol L^{-1}. The

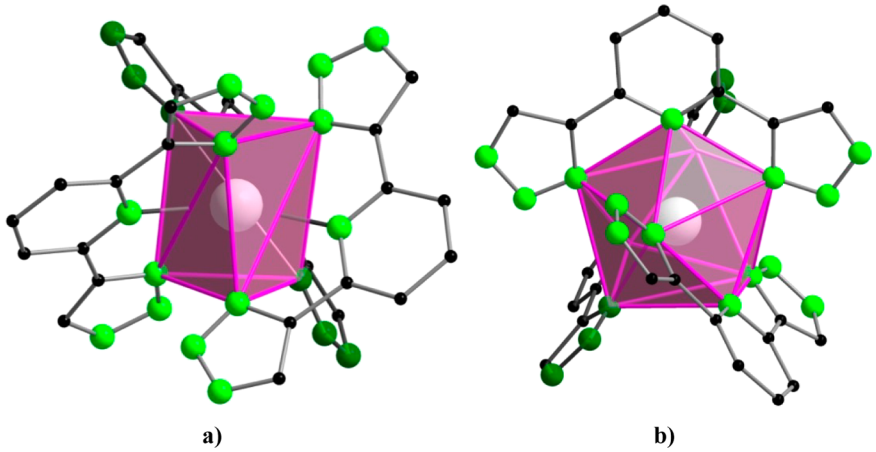

Figure 2. Coordination polyhedron of **1**. (a) By considering only the six nitrogen atoms of the triazole rings coordinate to the europium atom a trigonal prismatic coordination geometry (CN = 6) is formed. (b) Tricapped trigonal prismatic coordination geometry of all nine coordinating nitrogen atoms in total (CN = 9).

DOI: 10.1021/acs.inorgchem.5b00803
Inorg. Chem. 2015, 54, 7301–7308

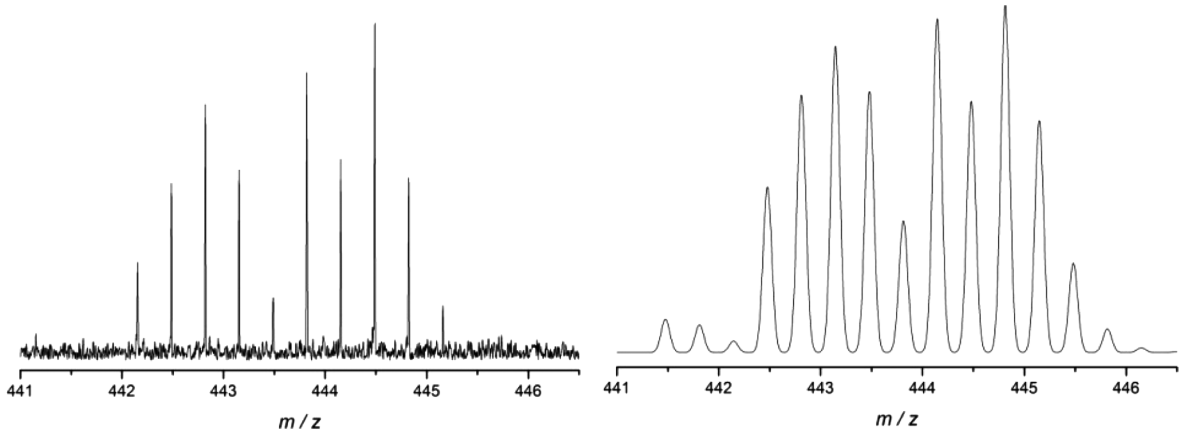

Figure 3. Cationic electrospray (ESI^+) spectrum of **2** in the region of m/z = 441−446 amu. The spectrum was recorded by using acetonitrile as a solvent (left). Calculated isotopic distribution of $[Sm(BTTP)_3]^{3+}$ (right).

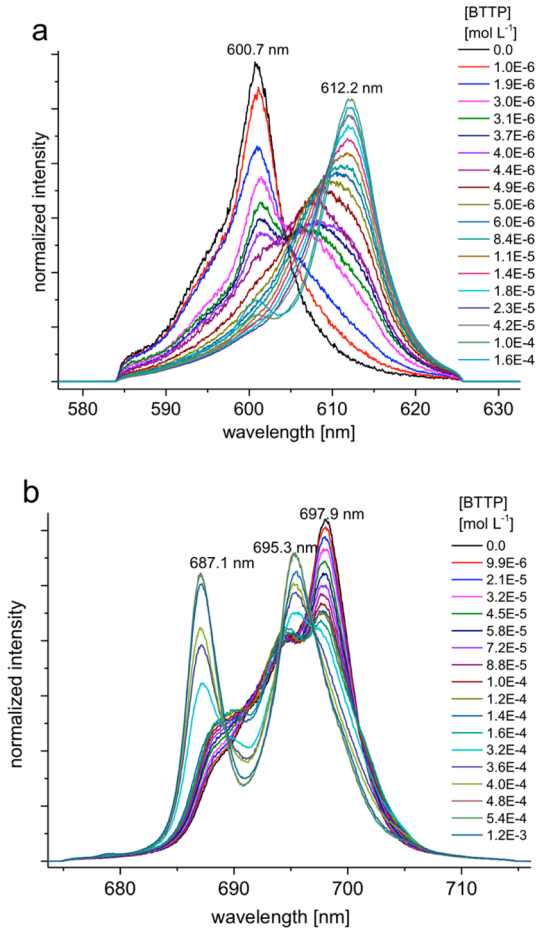

Figure 4. Normalized fluorescence spectra of (a) Cm(III) and (b) Eu(III) in MeCN (5.0 vol % H_2O) with increasing BTTP concentration. $[Cm(III)]_{ini}$ = 1.0 × 10^{-7} mol L^{-1}, $[Eu(III)]_{ini}$ = 4.0 × 10^{-5} mol L^{-1}. For a better overview not all titration steps are shown.

emission band of the second Cm(III) complex species (λ_{max} = 612.2 nm) is pronounced at [BTTP] > 8.4 μmol L^{-1}.

Eu(III) fluorescence bands only show a very weak bathochromic shift with changes in the inner coordination sphere. However, the characteristic splitting of the $^5D_0 \rightarrow {}^7F_4$ emission band is useful for distinguishing different Eu(III) complex species.[43,34] The formation of different Eu(III) complex species upon addition of BTTP was studied using the Eu(III) $^5D_0 \rightarrow {}^7F_4$ emission band. The development of this emission band at increasing [BTTP] is shown in Figure 4b.

The solvated Eu(III) metal ion shows an emission band at λ_{max} = 697.9 nm with three weak hypsochromically shifted shoulders at λ_{max} = 694.6, 691.6, and 688.6 nm. With increasing [BTTP] two new Eu(III) complex species are formed. The emission band of the first Eu(III) complex species shows three emission maxima at λ_{max} = 689.9, 693.2, and 701.8 nm. The emission band of the second Eu(III) BTTP complex species is characterized by two narrow and intensive emission peaks with maxima at 687.1 and 695.3 nm.

The relative distribution of the Cm(III) and Eu(III) complex species after each titration step was obtained by peak deconvolution of the fluorescence spectra using the emission bands of the different Cm(III) and Eu(III) complexes (see Figures S3 and S4, Supporting Information). To calculate concentration ratios the relative species compositions obtained from the fluorescence spectra must be corrected by the fluorescence intensity (FI) factors of the different Cm(III) and Eu(III) complex species. Relative FI factors are calculated as ratio of the FI of the metal complex species and the FI of a reference. As reference the corresponding solvated metal ion before addition of the BTTP ligand is used:

$$FI_{rel} = \frac{I_{(M(III)complexspecies)}}{I_{(M(III)solventspecies)}}$$

The Cm(III) and Eu(III) complex species show significantly higher FI values compared to the solvated metal ions. For the two Cm(III) complex species the following FI factors were determined: [Cm(III) complex species 1/$Cm(solv)^{3+}$] = 25 and [Cm(III) complex species 2/$Cm(solv)^{3+}$] = 60. For the Eu(III) complex species slightly lower FI factors were observed: [Eu(III) complex species 1/$Eu(solv)^{3+}$] = 4 and [Eu(III) complex species 2/$Eu(solv)^{3+}$] = 22.

Figure 5a shows the species distribution of the different Cm(III) complex species as a function of the BTTP ligand concentration. The ratio of the solvated Cm(III) decreases with addition of the BTTP ligand and is below 20% at [BTTP] ≥ 1.8 × 10^{-5} mol L^{-1}. The first Cm(III) complex species yet forms at low BTTP concentration. The ratio of the first Cm(III) complex species is >10% at [BTTP] > 5.0 × 10^{-6} mol L^{-1}. Furthermore, this complex species is the prevailing species in a small concentration range of 1.8 × 10^{-5} mol L^{-1} ≤ [BTTP] ≤ 4.2 × 10^{-5} mol L^{-1} with a maximum ratio of 59% at [BTTP]

DOI: 10.1021/acs.inorgchem.5b00803
Inorg. Chem. 2015, 54, 7301−7308

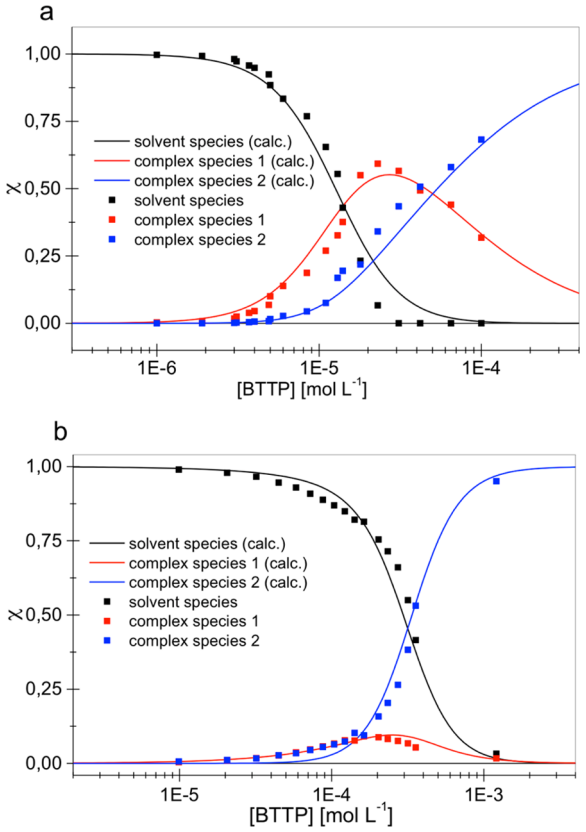

Figure 5. Species distribution of (a) the Cm(III) complex species as a function of [BTTP], $[Cm(III)]_{ini} = 1.0 \times 10^{-7}$ mol L^{-1} and (b) the Eu(III) complex species as a function of [BTTP], $[Eu(III)]_{ini} = 4.0 \times 10^{-5}$ mol L^{-1}. Lines calculated with the conditional stability constants (see Table 1).

$= 2.3 \times 10^{-5}$ mol L^{-1}. The second Cm(III) complex species is formed at higher BTTP concentration and becomes the dominating species at $[BTTP] > 5 \times 10^{-5}$ mol L^{-1}.

Because of the lower conditional stability constants (as shown below), Eu(III)-BTTP complex species are formed at higher BTTP concentration in comparison to the Cm(III) complexes (Figure 5b). The maximum relative ratio of the first Eu(III) complex species (10% at $[BTTP] = 1.6 \times 10^{-4}$ mol L^{-1}) is significantly lower compared to the first Cm(III) complex. The second Eu(III) complex species is the dominating species at $[BTTP] \geq 3.6 \times 10^{-4}$ mol L^{-1}. Furthermore, as shown in Figure 5 the Cm(III) and Eu(III) species distributions determined experimentally are in good agreement with the calculated species distribution using the conditional stability constants (see Table 1).

Identification of the Complex Species. The stoichiometry of the formed Cm(III) and Eu(III) complex species was determined by slope analysis. The formation of Cm(III) and Eu(III)-BTTP complex species is expressed by the following equilibrium:

$$M(solv)^{3+} + n\text{BTTP} \rightleftharpoons [M(\text{BTTP})_n]^{3+}$$

with M = Cm(III) or Eu(III).

Conditional stability constants of the formation of Cm(III) and Eu(III)-BTTP complex species are calculated from the experimental species distributions according to eq 1.

$$\beta_n' = \frac{[M(\text{BTTP})_n]^{3+}}{[\text{M(solv)}]^{3+}[\text{BTTP}]^n} \quad (1)$$

Rearrangement of eq 1 gives eq 2:

$$\log\left(\frac{[M(BTTP)_n]^{3+}}{[M(solv)]^{3+}}\right) = \log \beta_n' + n\cdot\log[BTTP] \quad (2)$$

Hence, there is a linear correlation between the logarithm of the concentration ratio $[M(BTTP)_n]^{3+}/[M(solv)]^{3+}$ and the logarithm of the free BTTP concentration with a slope of *n*. By linear regression of the double-logarithmic plots of the Cm(III) and Eu(III) complex species ratio versus the free ligand concentration slopes of 3.1 ± 0.3 for [Cm(III) complex species 2]/$[Cm(solv)]^{3+}$ and 3.2 ± 0.2 for [Eu(III) complex species 2]/$[Eu(solv)]^{3+}$ were determined. These results verify the formation Cm(III) and Eu(III) 1:3 complex species at increasing ligand concentration.

Slope analysis of the intermediate Cm(III) and Eu(III) complex species showed the formation of a 1:2 Cm(III)-BTTP complex (slope = 2.2 ± 0.2) and a 1:1 Eu(III)-BTTP complex (slope = 1.1 ± 0.1; Supporting Information, Figure S5). This behavior has already been observed with the HN_4bipy ligand.[34] A possible explanation for the observed formation of different intermediate complex species is the significantly better complexation performance of BTTP toward Cm(III) compared to that with Eu(III) (see Table 1), favoring the formation of the higher-coordinated intermediate complex species.

Determination of Stability Constants. Conditional stability constants for the formation of the Cm(III) and Eu(III) BTTP complexes were determined according to eq 1, using the experimental species distributions. Conditional stability constants for the complexation of Cm(III) with BTTP are $\log \beta'_2 = 9.7 \pm 0.2$ and $\log \beta'_3 = 14.0 \pm 0.3$. Stability constants of $\log \beta'_1 = 2.8 \pm 0.1$ and $\log \beta'_3 = 10.3 \pm 0.2$ are derived for the complexation of Eu(III) with BTTP. The stability constants are summarized in Table 1.

At first view these Cm(III) and Eu(III) $\log \beta'_3$ values are comparable to the stability constants obtained for BTP[37,44−46] and BPP,[29] but comparison of stability constants of various ligands determined at different conditions is a very difficult task. One needs to consider that the former stability constants were determined in acetonitrile, whereas the latter were determined in alcohol−water mixtures. As known from previous studies,[44] the solvent used and the amount of water present in the solvent mixture has a tremendous impact on determined thermodynamic data and can cause variation of the stability constants by several orders of magnitude.

Nevertheless, in good agreement with the results of BTP[37,44−46] and BTBP,[29] the formation of the 1:3 Cm(III) complex with BTTP is thermodynamically favored compared to the corresponding Eu(III) complex. The selectivity for Cm(III) over Eu(III) is ∼500, based on the difference of the Cm(III) and Eu(III) $\log \beta'_3$ values of 2.7 log units. Because of this high selectivity in monophasic titration experiments high separation factors are expected in biphasic liquid−liquid extraction. Hence, the experimental extraction performance of the BTTP and in

Table 1. Conditional Stability Constants for the Formation of $[Cm(BTTP)_n]$ and $[Eu(BTTP)_n]$ (n = 1−3) in MeCN (5.0 vol % H_2O)

metal ion	$\log \beta_1'$	$\log \beta_2'$	$\log \beta_3'$
Cm(III)		9.7 ± 0.2	14.0 ± 0.3
Eu(III)	2.8 ± 0.1		10.3 ± 0.2

DOI: 10.1021/acs.inorgchem.5b00803
Inorg. Chem. 2015, 54, 7301−7308

particular the separation factor $SF_{Am(III)/Eu(III)}$ (considering that Am(III) and Cm(III) have similar properties) was determined using liquid−liquid extraction tests (see below).

Protonation of 1:3 M(III) BTTP Complexes. Stability of the 1:3 complexes at high acidity is of importance as An(III)/Ln(III) separation processes will be performed from acidic solutions. Hence, the impact of increasing acidity on the stability of the formed complex species was investigated by progressively adding perchloric acid to equilibrated solutions of $[Cm(BTTP)_3]$ or $[Eu(BTTP)_3]$.

Normalized Cm(III) and Eu(III) fluorescence spectra at increasing acid concentrations are shown in the Supporting Information (Figures S6 and S7). As the solvent mixture contains a significant amount of acetonitrile, proton concentrations are noted as conditional pH values (pH_C). In contrast to the results of $[Cm(^nPr\text{-}BTP)_3]$[32] and in accordance with other 1:3 Cm(III)-N-donor complex species[32,30,34] a significant change of the emission spectra of the Cm(III) and Eu(III)-BTTP complexes was observed with increasing acidity.

In case of Cm(III) the emission band of the 1:3 complex species at λ_{max} = 612.2 nm was observed at a conditional pH value of 4.0. With increasing acidity the intensity of the emission band of $[Cm(BTTP)_3]$ decreased, and the emission band of the Cm(III) solvent species (λ_{max} = 600.7 nm) gained intensity. A similar behavior was observed for the Eu(III)-BTTP 1:3 complex. At an initial pH_C of 3.6 the Eu(III) $^5D_0 \rightarrow {}^7F_4$ emission band showed the characteristic splitting of the 1:3 complex species with two emission maxima at λ_{max} = 687.0 and 695.2 nm. Upon increasing acidity the splitting changed, displaying the characteristic splitting of the intermediate 1:1 complex species. Hence, the Cm(III)-BTTP and Eu(III)-BTTP 1:3-complex species are prone to decomplexation at higher proton concentration.

Slope analysis furthermore proved the exchange of one proton in the first decomplexation step from $[Cm(BTTP)_3]$ to the intermediate complex species $[Cm(BTTP)_2]$ and the subsequent exchange of two protons from $[Cm(BTTP)_2]$ to the Cm(III) solvent species. For decomplexation studies of $[Eu(BTTP)_3]$ slope analysis verified the exchange of two protons, forming $[Eu(BTTP)_1]$, the identical intermediate complex species observed in the course of the titration experiment (see above).

Liquid−Liquid Extraction. A high selectivity of BTTP for actinides(III) over lanthanides(III) when used as extracting agents was expected from the difference in Cm(III) and Eu(III) log β'_3 values of 2.7 log units. Unfortunately, no extraction of Am(III) or Eu(III) into the organic phase was observed, whether extracting into a solvent composed of BTTP in 1-octanol or into a solvent consisting of BTTP and 2-bromodecanoic acid in 1-octanol: distribution ratios for both Am(III) and Eu(III) were always below 0.001, meaning that less than 0.1% of the respective metal ions was extracted into the organic phase.

A qualitative correlation between extracting performance and complex stability had been observed for other N-donor ligands.[37,38,32,30,29] An explanation for the discrepancy between the rather high stability constants found for BTTP and its extraction performance may be given by the different solvents used for determining both the complex stabilities and the extraction properties: acetonitrile as a weakly coordinating solvent competes much less than more complexing solvents such as alcohols or water. However, acetonitrile was needed in the TRLFS studies for solubility reasons.

CONCLUSION

The coordination properties of 2,6-bis(1-(*p*-tolyl)-1*H*-1,2,3-triazol-4-yl)pyridine (BTTP) were examined and compared to results for similar but systematically varied ligands to understand the influence of the ligand geometry on coordination behavior. Two novel lanthanide complexes, namely, $[Ln(BTTP)_3](OTf)_3$ (Ln = Eu (**1**), Sm (**2**)), were prepared and structurally characterized. ESI-MS measurements of these compounds in acetonitrile revealed the retention of these complexes as triply charged cationic species $[Ln(BTTP)_3]^{3+}$ in solution.

Further information on the composition and stability of Cm(III)-BTTP and Eu(III)-BTTP complexes formed in solution were obtained using TRLFS. Two different Cm(III) complexes, a 1:2 and a 1:3 Cm(III)-BTTP complex, are formed in solution. For Eu(III) the formation of a 1:1 and a 1:3 Eu(III)-BTTP complex was observed. The following conditional stability constants for the 1:3 M(III)-BTTP complexes are determined: log β'_3 $[Cm(BTTP_3]$ = 14.0 ± 0.3 and log β'_3 $[Eu(BTTP)_3]$ = 10.3 ± 0.2. This pronounced selectivity is similar to that of other highly selective N-donor ligands such as BTP, BTBP, or BPP. However, BTTP is not able to extract from acidic aqueous solutions into an organic phase, probably due to its reduced complexation strength in solvents relevant to extraction.

Obviously, and in agreement with earlier studies,[28−30,32] any deviation from the triazine−pyridine-based molecule core as found in BTP (see Scheme 1) or BTBP results in a more or less pronounced decrease in complex stability and, consequently, performance as an extracting agent.

ASSOCIATED CONTENT

Supporting Information

Illustrated solid-state structure, ESI spectrum, emission spectra, double logarithmic plots, analysis of slope from plot of complex species ratio versus proton concentration. X-ray crystallographic files in CIF format are available for the structure determination of **1**. The Supporting Information is available free of charge on the ACS Publications website at DOI: 10.1021/acs.inorgchem.5b00803.

AUTHOR INFORMATION

Corresponding Authors

*E mail: roesky@kit.edu. (P.W.R.)
*E-mail: petra.panak@kit.edu. (P.J.P.)

Notes

The authors declare no competing financial interest.

ACKNOWLEDGMENTS

This work is supported by the German Federal Ministry of Education and Research (BMBF) under Contract Nos. 02NUK020A, 02NUK020B, and 02NUK020D.

REFERENCES

(1) IEA. *Key World Energy Statistics 2014;* International Energy Agency (IEA): Paris, France, 2014.

(2) Gompper, K.; Geist, A.; Geckeis, H. *Nachr. Chem.* **2010**, *58*, 1015−1019.

(3) Modolo, G.; Wilden, A.; Geist, A.; Magnusson, D.; Malmbeck, R. *Radiochim. Acta* **2012**, *100*, 715.

(4) Modolo, G. Actinide(III) Recovery from High Active Waste Solutions Using Innovative Partitioning Processes. In *Nuclear Energy*

DOI: 10.1021/acs.inorgchem.5b00803
Inorg. Chem. 2015, 54, 7301−7308

and the Environment; American Chemical Society: Washington, DC, 2010; Vol. *1046*, pp 89−105.
(5) OECD-NEA. *Advanced Nuclear Fuel Cycles and Radioactive Waste Management;* NEA No. 5990, OECD, Nuclear Energy Agency (NEA): Paris, France, 2006.
(6) OECD-NEA. *Potential Benefits and Impacts of Advanced Nuclear Fuel Cycles with Actinide Partitioning and Transmutation;* NEA No. 6894, OECD, Nuclear Energy Agency (NEA): Paris, France, 2011.
(7) Musikas, C.; Le Marois, G.; Fitoussi, R.; Cuillerdier, C. In *Properties and Use of Nitrogen and Sulfur Donors in Actinide Separations;* Navratil, J. D., Schulz, W. W., Eds.; ACS Symposium Series 117, ACS: Washington, DC, 1980; pp 131−145.
(8) Musikas, C.; Vitorge, P.; Pattee, D. Progress in Trivalent Actinide Lanthanide Group Separations. In *Proceedings of the International Solvent Extraction Conference (ISEC 1983)*; American Institute of Chemical Engineers, Denver, CO, 26 Aug 26−Sept 2, 1983; pp 6−8.
(9) Jarvinen, G. D.; Barrans, R. E.; Schroeder, N. C.; Wade, K. L.; Jones, M. M.; Smith, B. F.; Mills, J. L.; Howard, G.; Freiser, H.; Muralidharan, S. Selective Extraction of Trivalent Actinides from Lanthanides with Dithiophosphinic Acids and Tributylphosphate. In *Separation of f Elements;* Nash, K. L., Choppin, G. R., Eds.; Plenum Press: New York, 1995; pp 43−62.
(10) Modolo, G.; Odoj, R. *Solvent Extr. Ion Exch.* **1999**, *17*, 33−53.
(11) Ekberg, C.; Fermvik, A.; Retegan, T.; Skarnemark, G.; Foreman, M. R. S.; Hudson, M. J.; Englund, S.; Nilsson, M. *Radiochim. Acta* **2008**, *96*, 225−233.
(12) Kolarik, Z. *Chem. Rev.* **2008**, *108*, 4208−4252.
(13) Hudson, M. J.; Harwood, L. M.; Laventine, D. M.; Lewis, F. W. *Inorg. Chem.* **2013**, *52*, 3414−3428.
(14) Panak, P. J.; Geist, A. *Chem. Rev.* **2013**, *113*, 1199−1236.
(15) Case, F. H. *J. Heterocycl. Chem.* **1971**, *8*, 1043−1046.
(16) Kolarik, Z.; Müllich, U.; Gassner, F. *Solvent Extr. Ion Exch.* **1999**, *17*, 1155−1170.
(17) Drew, M. G. B.; Foreman, M. R. S. J.; Hill, C.; Hudson, M. J.; Madic, C. *Inorg. Chem. Commun.* **2005**, *8*, 239−241.
(18) Foreman, M. R. S.; Hudson, M. J.; Drew, M. G. B.; Hill, C.; Madic, C. *Dalton Trans.* **2006**, 1645−1653.
(19) Nilsson, M.; Ekberg, C.; Foreman, M. R. S.; Hudson, M.; Liljenzin, J. O.; Modolo, G.; Skarnemark, G. *Solvent Extr. Ion Exch.* **2006**, *24*, 823−843.
(20) Geist, A.; Hill, C.; Modolo, G.; Foreman, M. R. S. J.; Weigl, M.; Gompper, K.; Hudson, M. J.; Madic, C. *Solvent Extr. Ion Exch.* **2006**, *24*, 463−483.
(21) Lewis, F. W.; Harwood, L. M.; Hudson, M. J.; Drew, M. G. B.; Desreux, J. F.; Vidick, G.; Bouslimani, N.; Modolo, G.; Wilden, A.; Sypula, M.; Vu, T. H.; Simonin, J. P. *J. Am. Chem. Soc.* **2011**, *133*, 13093−13102.
(22) Bremer, A.; Whittaker, D. M.; Sharrad, C. A.; Geist, A.; Panak, P. J. *Dalton Trans.* **2014**, *43*, 2684−2694.
(23) Trumm, S.; Wipff, G.; Geist, A.; Panak, P. J.; Fanghänel, T. *Radiochim. Acta* **2011**, *99*, 13−16.
(24) Byrne, J. P.; Kitchen, J. A.; Gunnlaugsson, T. *Chem. Soc. Rev.* **2014**, *43*, 5302−5325.
(25) Hudson, M. J.; Boucher, C. E.; Braekers, D.; Desreux, J. F.; Drew, M. G. B.; Foreman, M. R. S.; Harwood, L. M.; Hill, C.; Madic, C.; Marken, F.; Youngs, T. G. A. *New J. Chem.* **2006**, *30*, 1171−1183.
(26) Trumm, S.; Geist, A.; Panak, P. J.; Fanghänel, T. *Solvent Extr. Ion Exch.* **2011**, *29*, 213−229.
(27) Halcrow, M. A. *Coord. Chem. Rev.* **2005**, *249*, 2880−2908.
(28) Girnt, D.; Roesky, P. W.; Geist, A.; Ruff, C. M.; Panak, P. J.; Denecke, M. A. *Inorg. Chem.* **2010**, *49*, 9627−9635.
(29) Bremer, A.; Ruff, C. M.; Girnt, D.; Müllich, U.; Rothe, J.; Roesky, P. W.; Panak, P. J.; Karpov, A.; Müller, T. J. J.; Denecke, M. A.; Geist, A. *Inorg. Chem.* **2012**, *51*, 5199−5207.
(30) Bremer, A.; Geist, A.; Panak, P. J. *Dalton Trans.* **2012**, *41*, 7582−7589.
(31) Bremer, A.; Geist, A.; Panak, P. J. *Radiochim. Acta* **2013**, *101*, 285−291.
(32) Beele, B. B.; Rüdiger, E.; Schwörer, F.; Müllich, U.; Geist, A.; Panak, P. J. *Dalton Trans.* **2013**, *42*, 12139−12147.
(33) A. Bardwell, D.; C. Jeffery, J.; L. Jones, P.; A. McCleverty, J.; Psillakis, E.; Reeves, Z.; D. Ward, M. *J. Chem. Soc., Dalton Trans.* **1997**, 2079−2086.
(34) Kratsch, J.; Beele, B. B.; Koke, C.; Denecke, M. A.; Geist, A.; Panak, P. J.; Roesky, P. W. *Inorg. Chem.* **2014**, *53*, 8949−8958.
(35) Meudtner, R. M.; Ostermeier, M.; Goddard, R.; Limberg, C.; Hecht, S. *Chem.—Eur. J.* **2007**, *13*, 9834−9840.
(36) Ruff, C. M.; Müllich, U.; Geist, A.; Panak, P. J. *Dalton Trans.* **2012**, *41*, 14594−14602.
(37) Trumm, S.; Panak, P. J.; Geist, A.; Fanghänel, T. *Eur. J. Inorg. Chem.* **2010**, 3022−3028.
(38) Trumm, S.; Lieser, G.; Foreman, M. R. S.; Panak, P. J.; Geist, A.; Fanghänel, T. *Dalton Trans.* **2010**, *39*, 923−929.
(39) Lang, C.; Pahnke, K.; Kiefer, C.; Goldmann, A. S.; Roesky, P. W.; Barner-Kowollik, C. *Polymer Chem.* **2013**, *4*, 5456−5462.
(40) Kiefer, C. F. Synthese und Charakterisierung palladiumhaltiger Metallopolymere sowie Darstellung Alkin-funktionalisierter NHC-Liganden und deren mehrkernige Münzmetallkomplexe. Dissertation, Karlsruhe Institute of Technology: Karlsruhe, Germany, 2014.
(41) Sheldrick, G. *Acta Crystallogr., Sect. A* **2008**, *64*, 112−122.
(42) Klenze, R.; Kim, J. I.; Wimmer, H. *Radiochim. Acta* **1991**, *52*−*53*, 97−103.
(43) Wilden, A.; Modolo, G.; Lange, S.; Sadowski, F.; Beele, B. B.; Skerencak-Frech, A.; Panak, P. J.; Iqbal, M.; Verboom, W.; Geist, A.; Bosbach, D. *Solvent Extr. Ion Exch.* **2014**, *32*, 119−137.
(44) Bremer, A.; Müllich, U.; Geist, A.; Panak, P. J. *New J. Chem.* **2015**, *39*, 1330−1338.
(45) Colette, S.; Amekraz, B.; Madic, C.; Berthon, L.; Cote, G.; Moulin, C. *Inorg. Chem.* **2002**, *41*, 7031−7041.
(46) Colette, S.; Amekraz, B.; Madic, C.; Berthon, L.; Cote, G.; Moulin, C. *Inorg. Chem.* **2004**, *43*, 6745−6751.

DOI: 10.1021/acs.inorgchem.5b00803
Inorg. Chem. 2015, 54, 7301−7308